DTI
Drug Target Insights 2025; 19: 108-115
ISSN 1177-3928 | DOI: 10.33393/dti.2025.3631
ORIGINAL RESEARCH ARTICLE

Antioxidant potential of a new macrocyclic bisbibenzyl and other compounds from *Combretum molle*: *in vitro* and docking analyses

Angele Fanta[1,3], Gaetan Bayiha Ba Njock[1], Amadou Dawe[2], Fawai Yakai[1], Jean Noël Nyemb[3], Herve Landry Ketsemen[4], Vincent Taira[1], Albert Wangso[1], Chantal Doudja[1], Dieudonne Emmanuel Pegnyemb[4], Benoit Loura[3]

[1]Department of Chemistry, Faculty of Science, University of Maroua, Maroua - Cameroon
[2]Department of Chemistry, Higher Teachers Training College, University of Maroua, Maroua - Cameroon
[3]Department of Refining and Petrochemistry, National Advanced School of Mines and Petroleum Industries, University of Maroua, Kaélé - Cameroon
[4]Department of Organic Chemistry, Faculty of Science, University of Yaoundé I, Yaoundé - Cameroon

ABSTRACT

Introduction: Free radicals are key contributors to several diseases, including cancer, inflammation, pain, and neurodegenerative disorders such as Alzheimer's disease. Due to the limitations and adverse effects of synthetic antioxidants, naturally occurring phytochemicals offer safer, more sustainable alternatives. This study investigates the antioxidant potential of twigs of *Combretum molle* R. Br. ex G. Don through integrated experimental and computational approaches.

Methods: Compounds were isolated using chromatographic methods, and their structures established by 1D- and 2D-NMR, HR-ESI-MS, and comparison with reported data. Antioxidant activity was assessed through DPPH radical scavenging and FRAP assays, while molecular docking against xanthine oxidase (PDB: 1FIQ) explored possible mechanisms beyond direct radical scavenging.

Results: A new macrocyclic bisbibenzyl derivative, combrebisbibenzyl A (**1**), was identified along with corosolic acid (**2**), maslinic acid (**3**), a mixture of asiatic acid (**4**) and arjunolic acid (**5**), combregenin (**6**), and *β*-sitosterol glucoside (**7**). The MeOH extract and EtOAc fraction showed notable DPPH scavenging activity (IC_{50} = 170.21 and 197.41 µg/mL) and strong reducing power (65.04 ± 1.07 and 67.42 ± 0.82 mM Vit C/g). Among the isolated compounds, combrebisbibenzyl A (**1**) displayed the strongest radical scavenging effect (IC_{50} = 175.64 µg/mL) and high reducing capacity (57.46 ± 0.42 mM Vit C/g). Docking indicated favorable interactions for all compounds, with combrebisbibenzyl A (**1**) showing the highest affinity (–9.1 kcal/mol), outperforming salicylate (–7.7 kcal/mol).

Conclusion: These findings support the traditional use of *C. molle* and highlight combrebisbibenzyl A (**1**) as a promising natural antioxidant with multi-mechanistic potential.

Keywords: Antioxidant activity, *Combretum molle*, Combrebisbibenzyl A, Macrocyclic bis-bibenzyl, Molecular docking

Introduction

Combretum molle R. Br. ex G. Don, a plant belonging to the Combretaceae family, is widely distributed from tropical to subtropical areas of Africa and Asia (1). Commonly known as soft-leaved *Combretum* in French, *C. molle* has been reported in African folk medicinal practices to treat abdominal disorders, leprosy, fever, snake bites, wounds, worm infections, and convulsions. It is also reported to possess hepatoprotective, antimalarial, antituberculosis, and anti-HIV properties (2-4).

Previous chemical investigations have reported the presence of alkaloids, triterpenes, steroids, tannins, bibenzyls, phenanthrenes, and saponins from some species of the genus *Combretum* (5-7). Several stilbenes, dihydrostilbenes, and their dimers isolated from *Combretum* species have demonstrated strong antioxidant potential (6-8). However, despite these reports, the isolation and investigation of macrocyclic bisbibenzyl derivatives from *C. molle* remain limited, representing a gap in understanding their structural diversity and bioactivity.

As a continuation of our investigation on plants of the Combretaceae family, a new macrocyclic bis-bibenzyl derivative, combrebisbibenzyl A (**1**), was isolated from the twigs of *C. molle*, together with six other known secondary metabolites. Given the reported antioxidant potential of *C. molle*

Received: August 19, 2025
Accepted: November 26, 2025
Published online: December 18, 2025

This article includes supplementary material

Corresponding authors:
Dawe Amadou; Bayiha Ba Njock Gaetan; Jean Noël Nyemb
email: amadoudawe@gmail.com; bayihagaetan@yahoo.fr; nyembjeannoel@gmail.com

extracts and some isolated compounds (3), and the documented activity of related bis-bibenzyl derivatives (4,6,7), we focused on elucidating the antioxidant activity of this newly isolated compound.

To explore potential mechanisms beyond direct radical scavenging, molecular docking studies were conducted targeting xanthine oxidase (XO) inhibition. XO (EC 1.17.3.2) is a molybdenum-containing flavoprotein that catalyzes the terminal steps of purine catabolism, specifically the oxidation of hypoxanthine to xanthine and subsequently to uric acid (9,10). Beyond its metabolic role, XO is a major source of reactive oxygen species (ROS), particularly superoxide anions and hydrogen peroxide, generated as byproducts during the enzymatic reaction with molecular oxygen (11,12). Excessive ROS production by XO contributes to pathological conditions such as ischemia-reperfusion injury, cardiovascular diseases, inflammation, and other oxidative stress-related disorders (11,13,14).

Salicylic acid (salicylate) has been extensively studied as a competitive XO inhibitor and is commonly used as a reference standard in enzymatic assays due to its well-characterized binding mechanism and stabilizing effect on the enzyme (9,15). The crystal structure of bovine milk xanthine oxidase (PDB ID: 1fiq) complexed with salicylate was selected as the target protein because of its high-resolution structural data and the availability of a well-defined active site with a co-crystallized competitive inhibitor (9). This computational approach allows for the prediction of binding affinities and identification of molecular interactions that may contribute to the antioxidant properties of the isolated compounds.

Experimental

General experimental procedures

Bruker MicroTOF was used for Mass spectra analysis. NMR spectra obtained on Bruker Avance DPX-300FT and Bruker Avance III HD 500 NMR spectrometer. Isolation of pure compounds was performed using Column chromatography (CC) on silica gel 60 (Merck, Darmstadt, Germany). Sephadex LH-20 (Merck, Darmstadt, Germany) was used for separation and purification. Thin-layer chromatography (TLC) was performed on Silica gel 60 F254 plates, and TLC spots were detected under UV-254-nm light. Bioactivity was determined using a 96-well microplate reader (SpectraMax 340PC, Molecular Devices, USA). Methanol, ethanol, n-hexane, ethyl acetate, ferrous chloride and copper (II) were obtained from E. Merck (Darmstadt, Germany). 2,2'-Diphenyl-1-picrylhydrazyl (DPPH), 2,4,6-tri-(2-pyridyl)-s-triazine (TPTZ) from Calbiochem. Ascorbic acid, butylhydroxytoluene (BHT) from Sigma Aldrich (Mumbai, India).

Plant material

Combretum molle twigs were harvested around Maroua in Northern Cameroon in October 2023, and the identified was done by comparison with a voucher specimen available in the National Herbarium of Cameroon under the reference number 6518/SRF/CAM.

Extraction and compound isolation

Around 3 kg of the air-dried twigs of *C. molle* were crushed and extracted with 20 L of methanol for 72 H to yield 167 g of crude extract. 150 g of this extract was dissolved in 10 L of water and partitioned with 5 L of EtOAc to afford 62 g of EtOAc extract (62 g). 55 g of the resulted EtOAc extract was subjected to column chromatography (CC) using silica gel and eluted with a gradient n-hexane-EtOAc (100:0 to 0:100, v/v) and EtOAc-MeOH gradient (100:0 to 0:100, v/v) to afford 156 fractions of 300 mL each, which were combined into 7 major fractions (A- G) based on their TLC profiles. Fraction E (2 g) was subjected to repeated silica gel CC using a gradient elution of n-hexane-EtOAc (100:0 to 0:100, v/v) to yield compound **1** (17.2 mg). Fraction F (8.6 g) was subjected to silica gel CC using a gradient elution of n-hexane-EtOAc (100:0 to 0:100, v/v), followed by CC over Sephadex LH-20 eluting with CH_2Cl_2-CH_3OH 50:50, v/v to afford compounds **2** (19.4 mg), **3** (15.8 mg) and a mixture of **4** and **5** (23.8 mg). Compound **7** (21.3 mg) precipitated from fraction G (1.5 g). The residue of fraction G (1.12 g) was subjected to silica gel CC and eluted with a gradient of CH_2Cl_2-CH_3OH to afford compound **6** (21.3 mg).

Spectroscopic data of Combrebisbibenzyl A (1)

$C_{32}H_{32}O_{10}$, White powder; ^{1}H NMR (500 MHz, $CDCl_3$): δ_H 7.73 (2H, s, H-6 and H-13'), 6.83 (2H, s, H-3 and H-14'), 6.44 (2H, d, *J* = 2.5 Hz, H-12 and H-1'), 6.33 (2H, d, *J* = 2.5 Hz, H-10 and H-5'), 5.62 (2H, s, 2, 13'-OH), 5.33 (2H, s, 13, 2'-OH), 3.91 (6H, s, 1,2'– OCH_3), 3.80 (6H, s, 11,6'– OCH_3), 2.72 (4H, m, H-8 and H-8') and 2.70 (4H, m, H-7 and H-7'). ^{13}C NMR (125 MHz, $CDCl_3$): δ_C 158.7 (C-11 and C-6'), 153.1 (C-13 and C-2'), 144.9 (C-1 and C-12'), 143.8 (C-2 and C-13'), 141.5 (C-14 and C-3'), 131.7 (C-5 and C-10'), 124.6 (C-4 and C-9'), 115.2 (C-9 and C-4'), 114.3 (C-3 and C-14'), 109.9 (C-6 and C-11'), 101.2 (C-10 and C-5'), 106.7 (C-12 and C-1'), 56.3 (1, 12'-OCH_3), 55.4 (11, 6'-OCH_3), 31.0 (C-8 and C-8') and 29.2 (C-7 and C-7'). HR-ESI-MS m/z 575.1930 $[M-H]^-$ (Calcd for $C_{32}H_{31}O_{10}$ 575.1917).

Antioxidant and molecular docking activities

DPPH radical scavenging activity

The DPPH radical scavenging activity was evaluated following a slightly modified version of the method reported by (16). In brief, 5 µL of each sample (at concentrations between 62.5 and 500 µg) was added to 95 µL of a 0.3 mM ethanolic DPPH solution in a 96-well microplate (Costar). The mixture was then incubated at 37°C for 30 minutes in the dark. After incubation, the absorbance was recorded at 515 nm using a microplate reader, with ethanol-treated wells serving as the control. Each sample was analyzed in triplicate. Butylhydroxytoluene (BHT) was employed as the positive control, while the ethanol-treated wells were used as the negative control. The percentage of DPPH radical scavenging activity was calculated using the following equation (17,18):

$$\text{DPPH}\cdot \text{ scavenging effect (\%)} = \frac{(\text{Ac} - \text{As}) \times 100}{\text{Ac}}$$

Where Ac = absorbance of control and As = absorbance of sample.

Ferric reducing power (FRAP) activity

In the presence of an oxidizing agent, the ferric-tripyridyltriazine complex ([Fe^{3+}–TPTZ]) is reduced to its ferrous form ([Fe^{2+}–TPTZ]) (19). The ferrous ion–chelating capacity was determined according to the method described by Benzie (20), with slight modifications. In brief, 3 mL of freshly prepared FRAP reagent was mixed with 100 µL of the sample solution (500 µg/mL in DMSO) and incubated at 37°C for 10 minutes. The absorbance of the resulting mixture was measured at 593 nm using a UV–visible spectrophotometer. Ascorbic acid, a well-established natural antioxidant, served as the positive control. The FRAP reagent was prepared by combining 5 mL of TPTZ solution (10 mM in 40 mM HCl), 50 mL of acetate buffer (0.3 M, pH 3.6), and 5 mL of freshly prepared $FeCl_3$ solution (20 mM). All assays were performed in triplicate, and results were expressed as millimoles of Vitamin C equivalents per gram of sample (mM Vit C/g).

Molecular Docking Analysis

Preparation of Ligands

The three-dimensional structures of all isolated compounds were constructed using Chem3D Pro 15.0 software (PerkinElmer, USA). The molecular structures were drawn based on their elucidated NMR and mass spectrometric data, and all ligands were energy-minimized using the MM2 force field to obtain stable conformations prior to docking calculations. The optimized structures were saved in Protein Data Bank (.pdb) format for subsequent molecular docking studies.

Preparation of Target Protein

The crystal structure of bovine milk xanthine oxidase complexed with salicylate (PDB ID: 1FIQ) was obtained from the Protein Data Bank (Online) (9). This particular structure was chosen as it represents the oxidase form with a well-defined active site geometry and contains salicylate as a competitive inhibitor, serving as an appropriate reference for comparative analysis. Protein preparation was carried out using AutoDockTools (ADT) version 1.5.6 (21). Prior to docking, all water molecules, ions, and the co-crystallized salicylate ligand were removed. Polar hydrogens were added, and Gasteiger and Kollman partial charges were assigned to all atoms. The protonation states of ionizable residues were adjusted to reflect physiological pH (7.4), followed by energy minimization to eliminate steric conflicts.

Molecular Docking Procedure

Molecular docking simulations were conducted using AutoDock Vina version 1.2.7 (22), which utilizes an advanced scoring function to evaluate intermolecular interactions, including hydrogen bonds, hydrophobic contacts, van der Waals forces, and electrostatic interactions. The docking grid was centered on the molybdenum-containing active site originally occupied by salicylate, with coordinates set at x = 24.642, y = 15.264, z = 108.210 and grid dimensions of 40 × 40 × 40 Å. This configuration encompassed both the salicylate binding pocket and the surrounding molybdopterin active site, allowing comprehensive exploration of potential ligand binding modes. To validate the docking protocol, salicylate was re-docked into the active site, confirming the reliability of the procedure. For each compound, 50 independent docking runs were performed to ensure thorough sampling of conformational space. Binding poses were ranked according to their predicted binding energies (kcal/mol), and the conformation with the lowest energy was selected for detailed interaction analysis.

FIGURE 1 - Xanthine oxidase RCSB: 1FIQ, in complex with salicylate (co-crystallized ligand shown in green) and its cofactors (shown in yellow).

Analysis of Molecular Interactions

Intermolecular interactions between the docked ligands and xanthine oxidase were analyzed and visualized using Discovery Studio Visualizer 2021 (Dassault Systèmes BIOVIA, USA). The analysis encompassed hydrogen bonds, hydrophobic interactions, π–π stacking, π–alkyl interactions, salt bridges, and other non-covalent contacts. Hydrogen bonds were defined as interactions with donor–acceptor distances ≤3.5 Å and angles ≥120°. Binding affinities were reported as binding energies (kcal/mol), with more negative values indicating stronger interactions. All observed interactions were

compared with those of the reference inhibitor salicylate to evaluate the relative binding potential of the test compounds.

Statistical analysis

Results expressed as mean ± SD (n = 3). The analysis was done by one-way ANOVA followed by a Newman-Keuls Multiple Comparison post-test using the Graph Pad Prism 6.0 software (Microsoft, USA). Differences at $p < 0.05$ were considered statistically significant.

Results and discussion

Compounds identification

Air-dried twigs of *C. molle* (3 kg) were extracted by maceration in methanol (20 L), yielding 167 g of crude extract. This extract was suspended in water and subsequently partitioned with ethyl acetate. From the resulting EtOAc fraction, 62 g was subjected to sequential column chromatography on silica gel and Sephadex LH-20, using gradients of n-hexane/EtOAc followed by EtOAc/MeOH, which led to the isolation of seven compounds (**1**–**7**). Compound **1**, designated combrebisbibenzyl A, was characterized as a new macrocyclic bisbibenzyl. The remaining six compounds were identified as corosolic acid (**2**), maslinic acid (**3**), a mixture of asiatic acid (**4**) and arjunolic acid (**5**) (23), combregenin (**6**) (24), and *β*-sitosterol glucoside (**7**) (25,26) (Fig. 2). The structures of all isolated compounds were determined through spectroscopic techniques and by comparison with previously reported data.

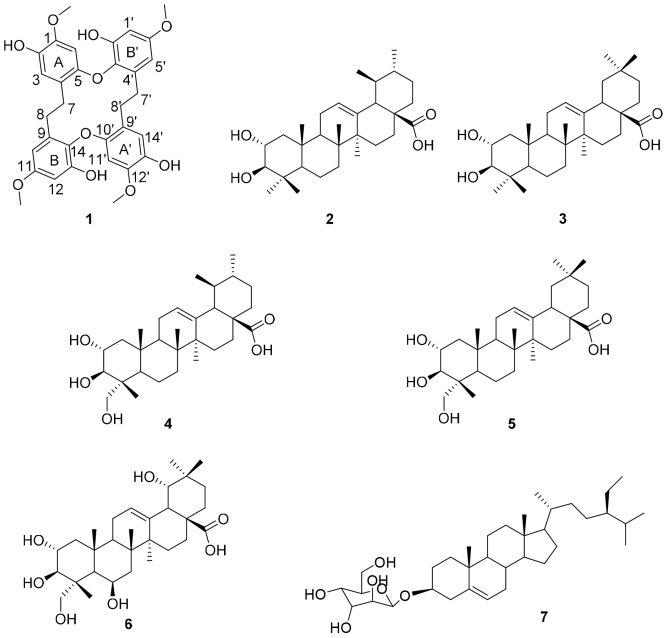

FIGURE 2 - Chemical structures of compounds **1-7** isolated from the twigs of *Combretum molle*.

Compound **1** was isolated as a white amorphous powder, and its molecular formula was determined to be $C_{32}H_{32}O_{10}$ based on its HR-ESI-MS data (Fig. S1), showing $[M-H]^-$ at *m/z* 575.1930 (calcd 575.1917 for $C_{32}H_{31}O_{10}$), which corresponds to seventeen degrees of unsaturation. The structure of compound **1** closely resembles a previously reported combrebisbibenzyl (27), with the primary distinction being that combrebisbibenzyl contains additional methoxy substituents compared to compound **1**. The ^{1}H NMR spectrum (Fig. S2) exhibited characteristic signals of two benzylic methylene groups, presenting as four aliphatic protons in multiplet patterns at δ_H 2.70 (2H) and 2.72 (2H) (28). Aromatic proton signals were observed at δ_H 6.33 (1H, d, *J* = 2.5 Hz) and 6.44 (1H, d, *J* = 2.5 Hz), indicative of a *meta*-coupled AB pattern on the B ring, along with δ_H 6.83 (1H, s) and 7.73 (1H, s) corresponding to *para*-substituted protons on the A ring (29). Two methoxy groups were detected at δ_H 3.80 (3H, s) and 3.91 (3H, s), and phenolic hydroxyl protons appeared at δ_H 5.33 (1H, s) and 5.62 (1H, s).^{13}C NMR and APT analyses (Figs S3 and S4) revealed 16 distinct carbon signals, including two aliphatic methylenes at δ_C 29.2 (C-7) and 31.0 (C-8), four methines at δ_C 114.3 (C-3), 109.9 (C-6), 101.2 (C-10), and 106.7 (C-12), and eight quaternary carbons, six of which were oxygenated, at δ_C 144.9 (C-1), 143.8 (C-2), 124.6 (C-4), 131.7 (C-5), 115.2 (C-9), 158.7 (C-11), 153.1 (C-13), and 141.5 (C-14). The two methoxy carbons resonated at δ_C 55.4 (11-OCH_3) and 56.3 (1-OCH_3). The relative positions of methoxy and hydroxyl groups were elucidated through HMBC correlations (Fig. S5). Cross-peaks between the hydroxyl proton at δ_H 5.62 (2-OH) and carbons C-1 (δ_C 144.9) and C-3 (δ_C 114.3), as well as between the methoxy protons at δ_H 3.91 (1-OMe) and C-1, confirmed their locations on the A ring. On the B ring, correlations of δ_H 5.33 (13-OH) with C-13 (δ_C 153.1) and δ_H 3.80 (11-OMe) with C-11 (δ_C 158.7) established the positions of the respective substituents. Additional HMBC correlations of aromatic protons further supported these assignments: H-3 (δ_H 6.83) correlated with C-1, C-2, C-4, and C-7, while H-6 (δ_H 7.73) showed correlations with C-1, C-2, C-4, and C-5 on the A ring. On the B ring, H-10 (δ_H 6.33) correlated with C-8, C-9, C-11, and C-12, and H-12 (δ_H 6.44) with C-10, C-11, and C-13. The HMBC correlations of H-7 (δ_H 2.70) with C-3, C-4, C-5, and C-8, and H-8 (δ_H 2.72) with C-7, C-9, and C-14, confirmed the linkage between the two benzene rings and established the dihydrostilbene skeleton (30). Accordingly, the dihydrobibenzyl moiety (**1a**) was deduced (Fig. 3), similar to combrebisbibenzyl. The seventeen degrees of unsaturation correspond to four aromatic rings and one additional unsaturation attributed to a symmetric macrocyclic junction between the two monomeric units of **1a** (31).

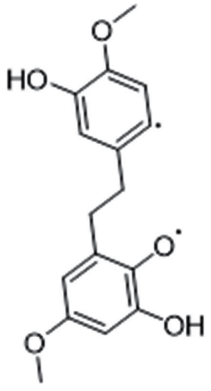

FIGURE 3 - Substructure **1a**.

Long-range HMBC correlations (27,31,32) (Fig. S6) between the proton signals H-6/H-11' (δ_H 7.73) and the quaternary carbon atoms C-4'/C-9 (δ_C 115.2) revealed the symmetric linkages between the two bibenzyl units at C-5–O–C-3' and C-14–O–C-10'. Based on these spectral data, the structure of compound **1** was identified as a novel bisbenzyl derivative, for which the name combrebisbibenzyl A has been proposed.

Antioxidant and molecular docking results

To establish a comprehensive antioxidant profile, we employed complementary approaches including the 2,2-diphenyl-1-picrylhydrazyl (DPPH) and Ferric Reducing Antioxidant Power (FRAP) assays, evaluating direct free-radical scavenging and metal-reduction capacities, respectively, combined with molecular docking against Xanthine oxidase (XO) to explore potential inhibition of enzymatic ROS production. The DPPH assay is widely used to evaluate antiradical activity through the ability of extracts or compounds to reduce the DPPH radical to its non-radical form (DPPH–H) and thus estimate their free-radical neutralizing potential in human-related systems (33). The FRAP assay, meanwhile, measures the capacity of antioxidants to donate electrons and reduce Fe^{3+} to Fe^{2+}, reflecting reducing power which complements radical-scavenging behavior, especially given that free radicals are often generated via redox-active metal catalysis (33). A positive correlation between DPPH and FRAP results has been well-documented, indicating that compounds able to donate hydrogen atoms (DPPH) also tend to act as efficient electron donors (FRAP) and thus share a common mechanistic basis (33,34). Inclusion of the XO assay further extends the evaluation from non-enzymatic antioxidant mechanisms to enzymatic ROS generation: XO catalyzes the oxidation of hypoxanthine/xanthine to uric acid with concomitant generation of superoxide radicals and hydrogen peroxide, so inhibition of XO represents a way to curb ROS at their source (35). Furthermore, compounds exhibiting strong radical-scavenging and reducing capacities often demonstrate XO inhibitory activity, suggesting a mechanistic link between non-enzymatic antioxidant potential and enzymatic ROS suppression (36,37). Thus, the combined use of DPPH, FRAP and XO-inhibition (or molecular docking thereof) provides a multi-faceted understanding of antioxidant mechanisms—covering hydrogen-atom transfer, electron-transfer/reduction power, and suppression of ROS-generating enzymes—and justifies our selection of these assays for the present study.

DPPH radical scavenging assay

In this study, the DPPH assay (Table 1) showed that the MeOH extract exhibited the highest free radical scavenging activity, with an IC_{50} value of 170.21 ± 1.12 µg/mL. This high activity can be attributed to its ability to extract phytochemical constituents, such as phenolic compounds and flavonoids, which are known to contribute to antioxidant effects. Statistically, there was no significant difference ($p < 0.05$) between the DPPH scavenging activity of the MeOH extract and the standard antioxidant BHT (IC_{50} = 170.86 ± 0.95 µg/mL). In contrast, the EtOAc extract showed weaker activity (IC_{50} = 197.41 ± 2.47 µg/mL), likely due to its lower content of phenolic compounds.

Among the isolated compounds, combrebisbibenzyl A (**1**) exhibited the highest scavenging activity (IC_{50} = 175.64 ± 1.36 µg/mL), followed by compound **7** (IC_{50} = 190.56 ± 1.42 µg/mL) and compound 6 (IC_{50} = 200.25 ± 1.51 µg/mL). The superior activity of compound **1** is likely related to the presence of phenolic hydroxyl groups in its structure, consistent with previous reports (12,14,27,38).

Ferric reducing power (FRAP) assay

The antioxidant reducing power of the samples was expressed as mmol vitamin C equivalents per gram of dry extract (mME Vit C/g). The calibration equation obtained from the vitamin C standard curve was $y = –0.001x + 2.605$ ($R^2 = 0.9976$), where y represents the absorbance measured at 593 nm and x denotes the concentration of vitamin C (µg/mL). The high correlation coefficient ($R^2 = 0.9976$) indicates excellent linearity and confirms the reliability of the calibration curve for quantifying the ferric-reducing antioxidant power (FRAP) of the test samples (20). The FRAP values of extracts and isolated compounds were calculated by interpolating their absorbance readings into this standard equation. This method is widely accepted for comparing the reducing potential of various antioxidant samples based on their equivalence to a standard electron donor such as vitamin C (39).

As shown in Table 1, the ethyl acetate (67.42 mME Vit C/g) and methanol (65.04 mME Vit C/g) extracts exhibited the highest metal-reducing capacities, suggesting that these extracts possess strong electron-donating abilities. Such activity may be attributed to the synergistic effects of phenolic and other redox-active phytochemicals capable of transferring electrons to reduce Fe^{3+} ions. Compounds **1** (57.46 mME Vit C/g) and **6** (59.79 mME Vit C/g) also demonstrated significant ferric-reducing potential compared to compound **7** (50.43 mME Vit C/g). The relatively higher reducing power of compounds **1** and **6** could be associated with the presence of free hydroxyl groups in their molecular structures, which facilitate electron transfer during redox reactions (20,39).

TABLE 1 - Variation of antioxidant activities of extracts and isolated compounds according to DPPH and FRAP test

Sample	DPPH		FRAP
	% inhibition	IC_{50} (µg/mL)	mMEVitC/g
1	67.42 ± 0.48^{c}	175.64 ± 2.87^{d}	57.46 ± 0.42^{d}
6	48.78 ± 0.58^{e}	200.25 ± 3.44^{a}	59.79 ± 0.65^{c}
7	62.29 ± 0.32^{d}	190.56 ± 2.61^{b}	50.43 ± 0.72^{e}
AcOEt Ex	63.42 ± 0.62^{d}	197.41 ± 2.47^{c}	67.42 ± 0.82^{a}
MeOH Ex	70.77 ± 0.55^{b}	170.21 ± 4.22^{e}	65.04 ± 1.07^{b}
BHT	74.12 ± 0.92^{a}	170.86 ± 2.19^{e}	-

AcOEt Ex: Ethyl Acetate Extract, MeOH Ex: Methanol Extract, BHT: Buthylhydroxytoluene. Values are expressed as Mean ± ET of 3 replicates per extracts and isolates. Means with different letters (a, b, c, d, e) in the same column are significant at P < 0.05

Molecular Docking Analysis

Molecular docking was performed to complement the experimental antioxidant assays by investigating a potential mechanism involving xanthine oxidase inhibition, while DPPH and FRAP measure direct antioxidant capacity, XO inhibition provides an indirect pathway by reducing the enzymatic generation of superoxide radicals. All tested compounds from Combretum molle exhibited favorable binding affinities to the XO active site, ranging from –8.0 to –9.1 kcal/mol (Table 2). Notably, the novel macrocyclic bisbibenzyl derivative combrebisbibenzyl A (compound 1) demonstrated the highest binding affinity (–9.1 kcal/mol), considerably superior to the reference inhibitor salicylate (–7.7 kcal/mol). A detailed comparative analysis reveals clear differences in binding modes between salicylate and compound **1**. While salicylate primarily interacts with ARG880 and PHE914 within the molybdopterin active site, compound **1** establishes a more extensive interaction network, engaging TYR592, LEU744, PHE798, and GLN1194 (Fig. 4). Its phenolic hydroxyl groups are optimally positioned for multiple hydrogen bonds. This broader and more deeply embedded interaction profile provides a plausible molecular basis for the superior binding affinity of compound **1**. Previous structure–activity relationship (SAR) studies of phenolic and polyphenolic inhibitors of XO underscore the importance of hydroxylation pattern (e.g., C5, C7 positions) and hydrogen-bonding with key residues in the enzyme for high inhibitory potency (40,41).

The consistent binding pattern across all compounds suggests competitive inhibition, as they occupy overlapping regions within the enzyme's active site. TYR592 emerges as a critical residue, forming hydrogen bonds with multiple compounds (**1**, **3**, **5**, **6**, **7**) in our series, supporting its mechanistic importance in XO inhibition. Importantly, the computational results correlate with experimental antioxidant activities: compounds **1** and **7**, both showing the strongest DPPH radical scavenging (IC_{50} = 175.64 and 190.56 µg/mL, respectively) and FRAP values (57.46 and 50.43 mmol Vit C-equivalents/g, respectively), also exhibit the highest XO binding affinities (–9.1 and –8.0 kcal/mol, respectively). This dual performance supports that combrebisbibenzyl A may exert antioxidant effects via multiple mechanisms: direct radical scavenging, metal-ion reduction, and suppression of enzymatic ROS generation. The macrocyclic structure of compound 1 appears to provide optimal geometry for engaging multiple key residues in XO's active site, while its phenolic hydroxyl groups facilitate crucial hydrogen bonding interactions in line with documented SAR of XO inhibitors (42,43).

Given this evidence, compound **1**'s high binding affinity supports its observed superior antioxidant activity and suggests that XO inhibition may play a significant role in its *in vitro* antioxidant profile. The comprehensive interaction network, favorable binding energy, and correlation with phenolic structural features position combrebisbibenzyl A as a promising multi-target antioxidant agent with scientific superiority over the reference compound salicylate.

TABLE 2 - Molecular docking results and binding interactions of isolated compounds with xanthine oxidase (PDB ID: 1fiq)

Compounds	Binding Energy (kcal/mol)	Key Interacting Residues and Interaction Types
SAL	–7.7	Salt Bridge - C chain: ARG880
		Conventional Hydrogen Bond - C chain: ARG880, THR1010
		Pi-Pi Stacked and Pi-Pi Shaped- C chain: PHE914, PHE1009
		Pi-Alkyl - C chain: ALA1079
1	–9.1	Conventional Hydrogen Bond - C chain: TYR592, LEU744
		Carbon and Pi-Donor Hydrogen Bond - C chain: GLN1194, GLU1196
		Pi-Sigma - C chain: LEU744
		Pi-Pi Shaped- C chain: PHE798
		Pi-Alkyl - C chain: TYR592, PHE798
2	–8.8	Conventional Hydrogen Bond - C chain: GLN1201
3	–8.2	Conventional Hydrogen Bond - C chain: TYR592, GLY1197
4	–8.0	Conventional Hydrogen Bond - C chain: PRO1230
		Unfavorable Donor-Donor - C chain: GLN1194
		Pi-Sigma - C chain: PHE1232
5	–8.0	Conventional Hydrogen Bond - C chain: GLN585, TYR592, MET794
		Carbon Hydrogen Bond - C chain: MET1038
6	–8.2	Conventional Hydrogen Bond - C chain: TYR592, MET1038
7	–8.0	Conventional Hydrogen Bond - C chain: GLN585, TYR592
		Alkyl - C chain: LEU744, VAL1200

Conclusion

This study reports the isolation of one novel macrocyclic bisbibenzyl derivative, combrebisbibenzyl A (**1**), along with six known triterpenoids from the twigs of *Combretum molle*. Experimental evaluation of antioxidant activity demonstrated that the EtOAc and MeOH extracts, as well as compounds **1**, **6**, and **7**, possess significant radical scavenging and metal-reducing capacities. Notably, combrebisbibenzyl A (**1**) exhibited the strongest activity, highlighting its potential as a bioactive natural antioxidant. These findings provide empirical evidence supporting the traditional use of *C. molle* in managing oxidative stress-related conditions, including infections and degenerative diseases. Molecular docking studies further suggest that combrebisbibenzyl

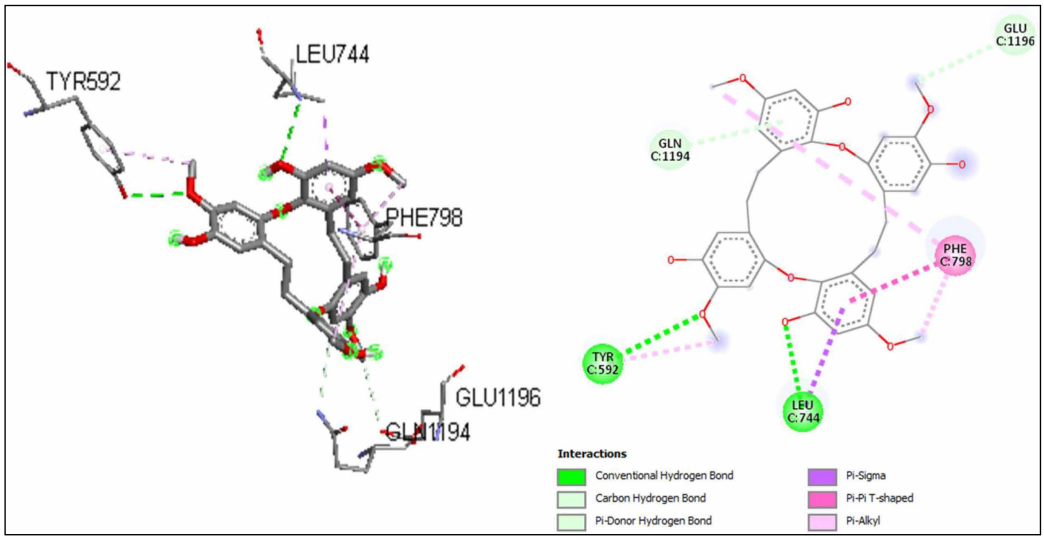

FIGURE 4 - 3D and 2D conformations of Combrebisbibenzyl A **(1)** in complex with 1fiq.

A may act as an effective xanthine oxidase inhibitor, with strong binding interactions involving key active site residues (TYR592, GLN1194, LEU744, ARG880). The complementary experimental and computational results indicate that the antioxidant potential of *C. molle* constituents may arise from both direct radical scavenging and inhibition of enzymatic reactive oxygen species generation. Overall, the data position *C. molle* extracts and isolated compounds as promising candidates for the development of natural antioxidant agents with potential applications in nutraceuticals, functional foods, and therapeutic interventions targeting oxidative stress-related disorders. Future research should focus on the detailed identification of specific bioactive phytochemicals, optimization of their bioavailability, and *in vivo* evaluation to advance their potential for drug development or dietary supplementation.

Acknowledgements

All the authors are grateful to the Laboratory of Biology, Faculty of Science, University of Maroua (Cameroon) for the biological experiments and the Department of Chemistry, Organic and Bioorganic Chemistry, Bielefeld University, Bielefeld, P.O. Box 100131, 33501 Bielefeld, Germany, for spectroscopic analysis of isolated compounds.

Disclosures

Conflict of interest: The authors declare that they have no known competing financial interests or personal relationships that could have appeared to influence the work reported in this paper.

Financial support: This research received no funding.

Data availability statement: The research data associated with this article are included within the article and in the supplementary material of this article.

Authors contribution: Conceptualization, A.D. and G.B.b.N.; Methodology, A.F. and A.D.; Software, J.N.N., H.L.K. and A.W.; Formal analysis, A.D., C.D., A.W. and G.B.b.N.; Investigation, A.F., G.B.b.N., A.W. and F.Y.; Data curation, A.D., C.D. and J.N.N.; Writing-original draft preparation, A.F., T.V., F.Y. and J.N.N.; Writing-review & editing, A.D. and J.N.N.; Project administration, D.E.P. and B.L.; Supervision, D.E.P. and A.D. All authors have read and agreed to the published version of the manuscript.

References

1. Viau CM, Moura DJ, Pflüger P, et al. Structural aspects of antioxidant and genotoxic activities of two flavonoids obtained from ethanolic extract of *Combretum leprosum*. Evid Based Complement Alternat Med. 2016;2016(1):9849134. CrossRef PubMed
2. Parusnath M, Naidoo Y, Singh M, et al. Antioxidant and antibacterial activities of the leaf and stem extracts of *Combretum molle* (R. Br. ex G. Don.) Engl. & Diels. Plants. 2023;12(9):1757. CrossRef PubMed
3. Dawe A, Saotoing P, Tsala DE, et al. Phytochemical constituents of *Combretum loefl*. (Combretaceae). Pharm Crop. 2013;4(1):38-59. CrossRef
4. Silén H, Salih EYA, Mgbeahuruike EE, et al. Ethnopharmacology, antimicrobial potency, and phytochemistry of African *Combretum* and *Pteleopsis* species (Combretaceae): a review. Antibiotics. 2023; *12*(2), 264. CrossRef
5. Ali IJ, Adonu CC, Okorie NH, et al. Phytochemical analysis, antioxidant and antimicrobial activities of the leaves of *Combretum bauchiense* Hutch & Dalziel (Combretaceae). SARJNP. 2023;6(3):248-260.
6. Asmaa SAE, Hanan AAT. Characterization of flavonoids from *Combretum indicum* L. growing in Egypt as antioxidant and antitumor agents. Egypt J Chem. 2023;66(13):2291-2305.
7. Silvère Gade I, Nyemb JN, Mahamat A, et al. A novel pentacyclic triterpene acid from the stem barks of *Combretum fragrans* F. Hoffm (Combretaceae). Nat Prod Res. 2024;38(8):1294-1301. CrossRef PubMed
8. Mathipa MM, Mphosi MS, Masoko P. Phytochemical profile, antioxidant potential, proximate and trace elements composition of leaves, stems and ashes from 12 *Combretum* spp. Used as Food Additives. Int J Plant Biol. 2022; 13(4), 561-578; CrossRef
9. Enroth C, Eger BT, Okamoto K, et al. Crystal structures of bovine milk xanthine dehydrogenase and xanthine oxidase: structure-based mechanism of conversion. Proc Natl Acad Sci USA. 2000;97(20):10723-10728. CrossRef PubMed

10. Rastelli G, Costantino L, Albasini A. A model of the interaction of substrates and inhibitors with xanthine oxidase. J Am Chem Soc. 1997; 119(13): 3007–3016. CrossRef
11. Battelli MG, Polito L, Bortolotti M, et al. Xanthine oxidoreductase-derived reactive species: physiological and pathological effects. Oxid Med Cell Longev. 2016;2016(1):3527579. CrossRef PubMed
12. Apak R, Özyürek M, Güçlü K, et al. Antioxidant activity/capacity measurement. 1. Classification, physicochemical principles, mechanisms, and electron transfer (ET)-based assays. J Agric Food Chem. 2016;64(5):997-1027. CrossRef PubMed
13. McCord JM. Oxygen-derived free radicals in postischemic tissue injury. N Engl J Med. 1985;312(3):159-163. CrossRef PubMed
14. Niccoli T, Partridge L. Ageing as a risk factor for disease. Curr Biol. 2012;22(17):R741-R752. CrossRef PubMed
15. Bergel F, Bray RC. Stabilization of xanthine oxidase activity by salicylate. Nature. 1956;178(4524):88-89. CrossRef PubMed
16. Gulcin I, Alwasel SH. DPPH radical scavenging assay. Processes (Basel). 2023;11(8):2248. CrossRef
17. Baliyan S, Mukherjee R, Priyadarshini A, et al. Determination of antioxidants by DPPH radical scavenging activity and quantitative phytochemical analysis of *Ficus religiosa*. Molecules. 2022;27(4):1326. CrossRef PubMed
18. Parusnath M, Naidoo Y, Singh M, et al. Phytochemical composition of *Combretum molle* (R. Br. ex G. Don.) Engl. & Diels leaf and stem extracts. Plants. 2023;12(8):1-19. CrossRef PubMed
19. Yaya JAG, Nyemb JN, Olboungou NM, et al. Antiradical, antibacterial activities and in silico molecular docking of ethyl-*β*-D-fructofuranoside from hydro-ethanolic crude extract of *Erythrina excelsa* stem bark. Plant Biosyst. 2025;159(4): 768-777. CrossRef
20. Benzie IFF, Strain JJ. The ferric reducing ability of plasma (FRAP) as a measure of "antioxidant power": the FRAP assay. Anal Biochem. 1996;239(1):70-76. CrossRef PubMed
21. Morris GM, Huey R, Lindstrom W, et al. AutoDock4 and AutoDockTools4: automated docking with selective receptor flexibility. J Comput Chem. 2009;30(16):2785-2791. CrossRef PubMed
22. Trott O, Olson AJ. AutoDock Vina: improving the speed and accuracy of docking with a new scoring function, efficient optimization, and multithreading. J Comput Chem. 2010;31(2):455-461. CrossRef PubMed
23. Facundo VA, Rios KA, Medeiros CM, et al. Arjunolic acid in the ethanolic extract of *Combretum leprosum* root and its use as a potential multi-functional phytomedicine and drug for neurodegenerative disorders: anti-inflammatory and anticholinesterasic activities. J Braz Chem Soc. 2005; 16 (6b). CrossRef
24. Ponou B, Barboni L, Teponno R, et al. Polyhydroxyoleananetype triterpenoids from *Combretum molle* and their antiinflammatory activity. Phytochem Lett. 2008;1(4):183-187. CrossRef
25. De Leo M, De Tommasi N, Sanogo R, et al. Triterpenoid saponins from *Pteleopsis suberosa* stem bark. Phytochemistry. 2006;67(24):2623-2629. CrossRef PubMed
26. Nyemb JN, Djankou MT, Talla E, et al. Antimicrobial, *α*-glucosidase and alkaline phosphatase inhibitory activities of bergenin, the major constituent of *Cissus populnea* roots. Med Chem (Los Angeles). 2018;8(2):426-430. CrossRef
27. Yakai F, Dawe A, Manshuk I, et al. Antioxidant and antibacterial effects of a new macrocyclic bis(bibenzyl) ether from *Combretum molle* (Combretaceae). Z Naturforsch C J Biosci. 2024;79(11-12):377-385. CrossRef PubMed
28. Cioffi G, Montoro P, De Ugaz OL, et al. Antioxidant bibenzyl derivatives from Notholaena nivea Desv. Molecules. 2011;16(3):2527-2541. CrossRef PubMed
29. Chaofeng Z, Min W, Ping L, et al. A new bibenzyl compound from *Dendrobium gratiosissmum*. ChemInform. 2008;39(19). CrossRef
30. Karatoprak GŞ, Küpeli Akkol E, Genç Y, et al. Combretastatins: an overview of structure, probable mechanisms of action and potential applications. Molecules. 2020;25(11):1-33. CrossRef PubMed
31. Asakawa Y, Toyota M, Tori M, et al. Chemical structures of macrocyclic bis(bibenzyls) isolated from liverworts (Hepaticaea). J Spectrosc. 2000;14(4):149-175. CrossRef
32. Araya-Maturana R, Pessoa-Mahana H, Weiss-López B. Very long-range correlations ($^{n}J_{C,H}$ n > 3) in HMBC spectra. Nat Prod Commun. 2008;3(3):445-450. CrossRef
33. Clarke G, Ting KN, Wiart C, et al. High correlation of 2,2-diphenyl-1-picrylhydrazyl (DPPH) radical scavenging, ferric reducing activity potential and total phenolics content indicates redundancy in use of all three assays to screen for antioxidant activity of extracts of plants from the Malaysian rainforest. Antioxidants (Basel). 2013;2(1):1-10 CrossRef PubMed
34. Han C, Shi H, Cui C, et al. Strain-specific benefits of *Bacillus* on growth, intestinal health, immune modulation, and ammonia-nitrogen stress resilience in hybrid grouper. Antioxidants (Basel). 2024;13(3):317. CrossRef PubMed
35. Noda M, Kikuchi C, Tarui R, et al. Effects of xanthine oxidoreductase inhibitors on reactive oxygen species produced in vitro from xanthine oxidase. BPB Reports. 2023;6(6):189-192. CrossRef
36. Ahmad AR, Elya B, Mun'im A. Antioxidant activity and isolation of xanthine oxidase inhibitor from *Ruellia tuberosa* L. leaves. Pharmacogn J. 2017;9(5):607-610. CrossRef
37. Ozyürek M, Bektaşoğlu B, Güçlü K, et al. Measurement of xanthine oxidase inhibition activity of phenolics and flavonoids with a modified cupric reducing antioxidant capacity (CUPRAC) method. Anal Chim Acta. 2009;636(1):42-50. CrossRef
38. Nyemb JN, Ndoubalem R, Talla E, et al. DPPH antiradical scavenging, anthelmintic and phytochemical studies of *Cissus poulnea* rhizomes. Asian Pac J Trop Med. 2018;11(4):280-284. CrossRef
39. Apak R, Güçlü K, Ozyürek M, et al. Novel total antioxidant capacity index for dietary polyphenols and vitamins C and E, using their cupric ion reducing capability in the presence of neocuproine: CUPRAC method. J Agric Food Chem. 2004;52(26):7970-7981. CrossRef PubMed
40. Liu X, Wu D, Liu J, et al. Characterization of xanthine oxidase inhibitory activities of phenols from pickled radish with molecular simulation. Food Chem X. 2022;14:100343. CrossRef PubMed
41. Li X, Wang J. Structure–activity relationships and changes in the inhibition of xanthine oxidase by polyphenols: a review. Food Chem Adv. 2022;15:100121.
42. Mehmood A, Li J, Rehman M, et al. Xanthine oxidase inhibitory study of eight structurally diverse phenolic compounds. Front Nutr. 2022;9:966557. CrossRef
43. Chen Y, Gao F, Wu X, et al. Computationally exploring novel xanthine oxidase inhibitors using docking-based 3D-QSAR, molecular dynamics, and virtual screening. New J Chem. 2020;44(44):19276-19287. CrossRef